Available online at www.sciencedirect.com

SCIENCE DIRECT

Cement and Concrete Research 35 (2005) 999–1007

Cement and Concrete Research

Theoretical assessment of the limit strengthening criterion of strengthened bridge decks based on failure characteristics

Jongsung Sim[a], Hongseob Oh[a,*], Jae-Myung Yu[b], Jae-Won Shim[c]

[a]*Department of Civil and Environmental Engineering, Hanyang University, 1271 Sa1-dong, Ansan 425-791, South Korea*
[b]*Pyung-Hwa Engineering Corporation, South Korea*
[c]*Highway and Transportation Technology Institute, 50-5, Dontanmyun, Hwasung, 445-812, South Korea*

Received 21 April 2004; accepted 20 August 2004

Abstract

The dominant failure modes of bridge deck are either flexure-shear or punching shear. Bridge decks strengthened with fiber reinforced polymers (FRPs) have an increased punching shear strength as well as improved flexural strength. This transforms the failure mode from biaxial bending to punching shear. Therefore, it is desirable to design the strengthened bridge deck so that it fails due to similar ductile behavior and with similar failure patterns as unstrengthened bridge decks, even though the ultimate strength of a strengthened deck with external reinforcements is much greater than its punching shear strength. For this reason, the concept of a strengthening limit criterion is introduced in this paper to ensure that strengthened decks have ductile dominant failure modes. The concept of failure mode transition, which is dependent on the amount of strengthening, is introduced in the practical design procedure, and a criterion for selecting the strengthening ratio is developed.

Keywords: Fiber reinforced polymers; Bridge deck; Strengthening limit criterion; Structural strengthening

1. Introduction

Permanent deformations of decks caused by excessive repeated heavy traffic loads are one of the main deterioration phenomena leaded to failure of decks. The deteriorated bridge decks then fail either due to spalling of the concrete or a punching shear failure [1–6]. During the last decade, many studies have focused on repair and rehabilitation techniques for concrete structures, and more efficient strengthening techniques and design methods have been reported [2,6]. The authors have verified the failure mechanisms of bridge decks strengthened with fiber reinforced polymers (FRPs) based on static and fatigue test results, and proposed an efficient strengthening method and simplified flexural design procedure [7–9]. In previous studies, the authors have also reported that two-directional strengthening with FRP strips is the most effective strengthening technique; it increases the ultimate strength of the deck and the fatigue resistance. A simplified strengthening design procedure to control brittle failures and extend the life cycle of deteriorated decks has also been developed.

The typical failure patterns of strengthened decks have been classified as bending failures due to the flexural stress and punching shear failures due to the shear stress. However, it is difficult to estimate the optimal amount of strengthening for a deteriorated bridge deck, because practical analysis methods for strengthened decks have not yet been developed. Oh and Sim [9] used static tests with various FRPs to experimentally assess the enhanced punching shear strength of strengthened decks. They proposed a modified yield line analysis for strengthened decks, which considered the failure characteristics of the FRPs. To prevent compressive failures, Bae [10] derived a maximum strengthening ratio, which corresponded to the existing reinforcement ratio, based on test results of strengthened beams.

In this study, we contemplate why the failure patterns of bridge decks strengthened with various materials change

* Corresponding author. Tel.: +82 31 400 5208; fax: +82 31 418 7430.
E-mail address: opera69@chol.com (H. Oh).

0008-8846/$ - see front matter © 2004 Elsevier Ltd. All rights reserved.
doi:10.1016/j.cemconres.2004.08.017

Nomenclature

a	the loading width in the transverse direction
a_b	the depth of equivalent stress block
A_p	the area of strengthening material in unit width
A_s	the area of reinforcing steel bars in unit width
b	the loading width in the longitudinal direction
b_1	the width of beam section
b_p	the width of strengthening material
c_b	the depth of neutral axis
C_p	the compressive force of concrete corresponding to the strengthening materials
C_s	the compressive force of concrete corresponding to the steel bars
d	the effective depth of beam section
D	the diameter of the anchor bolt
d'	the effective depth of compression reinforcement
d_a	the maximum aggregate size
E_p	the elastic modulus of the strengthening material
E_s	the elastic modulus of reinforcing steel bar
f'_c	the compressive strength of the concrete
f_p	the ultimate strength of the strengthening material
f_p^*	the maximum strength of the strengthening material
f_{psy}	the stress of the strengthening material when the reinforcements yield
f_s	the stress of steel bar
f_{sp}	the spalling strength of concrete
f_t	the tensile strength of the concrete
f_y	the yield strength of steel bar
h_p	the height of beam section
l	the clear span of deck panel
l_a	the length of anchor bolt
m_n	the positive yield moment per unit width
m'_n	the negative yield moment per unit width
n_p	the ratio of E_p to E_s
P_{anchor}	the resistance of the anchor bolts
P_{bond}	the pull-out strength by bonding effect
P_{cone}	the pull-out strength by concrete cone
P_{c1}	the vertical component of the tensile force from the compression side to $0.1d$
P_{c2}	the vertical component of the tensile force from $0.1d$ to d
P_{c3}	the vertical component of the tensile force from d to h_p
P_{dow}	the dowel action of the flexural reinforcement
$P_{pun,s}$	the punching shear strength of deck panel
$P_{y,s}$	the flexural strength of deck panel
r_s	the radius of an equivalent column circle in a slab-column system
t_p	The thickness of strengthening material
T_p	the tensile force of strengthening materials
T_s	the tensile force of steeel reinforcing bars
u	the length of the unbonded part of anchor bolt
u_s	the bond strength
x_c	the critical depth of the first cone failure of anchor bolt
$\sum^{bars} A_s$	the sum of the cross sectional areas of the reinforcing steel bars embedded in the punching cone
β	the tan ϕ in failure surface of anchor bolt
β_1	0.85
ε_p	the ultimate strain of the strengthening material
ε_p^*	the maximum strain of the strengthening material
ζ	the ratio of f_s to f_y
η	the coefficient of loading area effect
θ_1	the first inclination angle of the failure surface from the top of the compression side to d'
θ_2	the second inclination angle from d' to d
θ_3	the third inclination angle from d to h_p
λ	the experimental coefficient for strength reduction factor of strengthening material (0.72)
μ	The efficient of orthotropy
μ_a	the coefficient of aggregate size effect
ξ	the coefficient of reinforcement effect
ρ_s	the reinforcement ratio
$\rho_{s,b}$	the balanced reinforcement ratio
$\rho_{s,max}$	the maximum reinforcement ratio
ρ_{equi}	the equivalent reinforcement ratio of FRP
ρ_p	the strengthening ratio
$\rho_{p,b}$	the balanced strengthening ratio
$\rho_{p,max}$	the maximum strengthening ratio
ϕ	the apex angle of the cone
ϕ_s	the diameter of steel bar
$\cot \psi/2\sqrt{\frac{m_n}{m_n'}}$	

from flexure to shear. We also use yield line and punching strength analyses to analyze the theoretical flexural and shear strength of strengthened prototype decks according to the amount of strengthening. From this analytical approach, a strengthening limit criterion is proposed for the design of strengthening in bridge decks. A design criterion that can be used to select an appropriate strengthening ratio that ensures the ductile failure of a strengthened deck is also suggested from the results of a parametric study of the relationship between the reinforcement ratio and the strengthening limit criterion.

2. Failure criteria of strengthened decks

2.1. Maximum strengthening ratio

Without strain hardening, most strengthening materials, such as FRP plastics, have a perfect elastic behavior up to their ultimate strain. Therefore, the balanced steel reinforcement ratio and balanced strengthening ratio of a strengthened beam indicate when the tensile failure of the FRP reinforcements and compressive failure of the concrete occur at the same time, as shown in Fig. 1. The relationship between the reinforcement ratio $\left(\rho_s = \frac{A_s}{b_1 d}\right)$, strengthening ratio $\left(\rho_p = \frac{A_p}{b_1 h_p}\right)$, and failure pattern of a strengthened concrete member is depicted in Fig. 2.

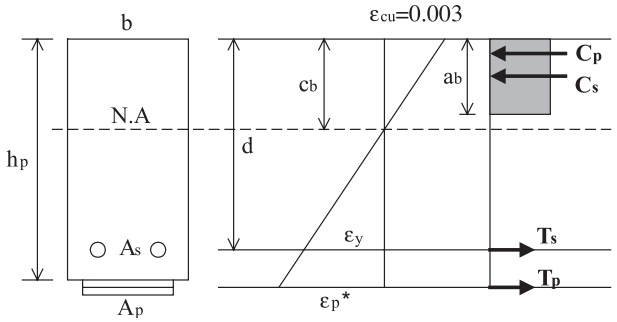

Fig. 1. Equilibrium state of strengthened R/C beam.

A typical compressive failure that results in crushed concrete and occurs without either the rebar or the FRPs failing, which would arise in an over-strengthened member, is indicated by 'Region C' in Fig. 2. A section that has a reinforcement ratio located in 'Region A' has a dominant ductile failure mode when the strengthened material ruptures after the rebar yields but the concrete is not crushed. This is defined within the range of the maximum steel reinforcement ratio $\rho_{s,max}$ and the maximum strengthening ratio $\rho_{p,max}$.

The boundary of the above two failure modes is defined as a balanced failure, 'Region B' in Fig. 1, in which the strengthening material ruptures after the rebar yields and the concrete is crushed at the same time. The reinforcement ratio and strengthening ratio of a balanced failure are indicated by $\rho_{s,b}$ and $\rho_{p,b}$, respectively. According to previous studies, the strengthening ratio selected in the design process should be located in Region A [7,10]. From the equilibrium condition shown in Fig. 1, the balanced steel reinforcement ratio and strengthening ratio of a strengthened section can be derived as follows. First, C_s=T_s, where C_s is the compressive force of the concrete corresponding to the tensile force of steel reinforcing bar, T_s, so that

$$0.85^2 f_c' c_b b_1 = f_y A_s \tag{1}$$

where f'_c is the compressive strength of the concrete, b is the unit width of the beam or slab, and A_s is the area of the steel bars. Eq. (1) can be divided by $b_1 d f_y$ so that

$$\rho_{s,b} = \frac{A_s}{b_1 d} = \frac{0.85^2 f_c' c_b b_1}{b_1 d f_y} \tag{2}$$

The depth of the equivalent stress block a_b=$\beta_1 c_b$, where β_1 is 0.85 for concrete with $f'_c \leq 27.6$ MPa. The depth of the neutral axis c_b can be determined from a strain diagram so that

$$c_b = \frac{0.003}{(0.003 + \varepsilon_p^*)} h_p \tag{3}$$

where 0.003 is the compressive strain of the concrete at failure, ε_p^* is the maximum strain of the strengthening material that is actually bonded to the concrete surface on the tension side, and h_p is the height of the beam or slab. The value of ε_p^* is slightly different from the ultimate strain of the strengthening material, ε_p. Substituting Eq. (3) into Eq. (2), the balanced reinforcement ratio is

$$\rho_{s,b} = \frac{0.00217 f_c'}{(0.003 + \varepsilon_p^*) f_y} \frac{h_p}{d} \tag{4}$$

In the same manner, the balanced strengthening ratio can be derived from the relation C_p=T_p, where C_p is the compressive force of the concrete that corresponds to the tensile force of the strengthening material (T_p=f_p×A_p). The balanced strengthening ratio is

$$\rho_{p,b} = \frac{0.00217 f_c'}{(0.003 + \varepsilon_p^*) f_p^*} \frac{h_p}{d} \tag{5}$$

According to the previous experimental studies, the maximum strain of the carbon fiber sheet (CS), ε_p^*, i.e., one which is bonded to the concrete surface, is 0.95% to 1.14%, while the ultimate strain of the CS, ε_p, is 1.4% to 1.5%. There is a difference of 0.72% between the maximum strain and the ultimate strain, which introduces the

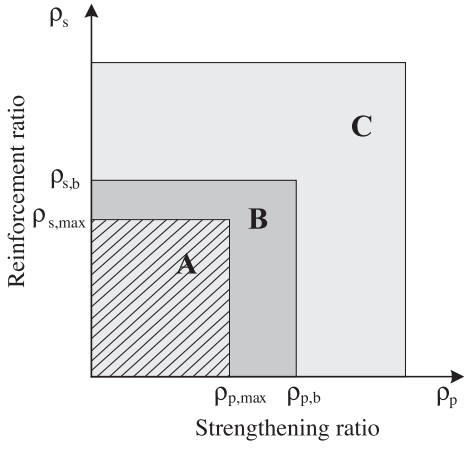

Domain	Failure aspect
A	Under reinforcement
B	FRP rupture or concrete crushing
C	Over reinforcement

Notes) ρ_s -steel reinforcement ratio,
$\rho_{s,b}$ -balanced steel reinforcement ratio,
$\rho_{s,max}$ -maximum steel reinforcement ratio,
ρ_p -strengthening ratio,
$\rho_{p,b}$ -balanced, maximum strengthening ratio
$\rho_{p,max}$ -maximum strengthening ratio

Fig. 2. Strengthening design limitation.

parameter λ=0.72 (for CS) into the equations. Therefore, the balanced reinforcement and strengthening ratios are

$$\rho_{s,b} = \frac{0.00217 f_c'}{(0.003 + \lambda\varepsilon_p) f_y} \frac{h_p}{d} \tag{6a}$$

$$\rho_{p,b} = \frac{0.00217 f_c'}{(0.003 + \lambda\varepsilon_p) \lambda f_p} \frac{h_p}{d} \tag{6b}$$

and the maximum reinforcement and strengthening ratios are assumed as follows.

$$\rho_{s,max} = 0.75\rho_{s,b} \text{ and } \rho_{p,max} = 0.75\rho_{p,b} \tag{7}$$

2.2. Failure patterns of strengthened decks

The structural response of strengthened bridge decks must be carefully considered in the design of strengthening because bridge decks receive vehicle loads. A strengthened bridge deck must fail after yield of rebars, even if it fails due to punching shear. However, if the yield strength ($P_{y,s}$) is placed above the punching strength ($P_{pun,s}$) in the load-displacement relationship, as illustrated in Fig. 3, the deck is unlikely to behave in a ductile manner; rather, a brittle failure will occur due to punching shear. This indicates that 'Region A', which covers the range of flexural failures for a deck panel, actually consists of flexural failures and punching shear failures. Therefore, to ensure the ductile failure pattern of strengthened deck, strengthening materials of only limited amount that is assessed in strengthening design, should be applied. In this study, we use yield line theory and a punching shear model to assess the theoretical ultimate strength of a strengthened deck.

2.3. Yield line theory

Oh et al. [8] derived a theoretical method to determine the flexural strength of strengthened decks. The assumed failure pattern of a strengthened deck is illustrated in Fig. 4. The flexural strength of the deck can be calculated from the following equations. The flexural strengths $P_{y,s}$ that correspond to each yield line pattern are

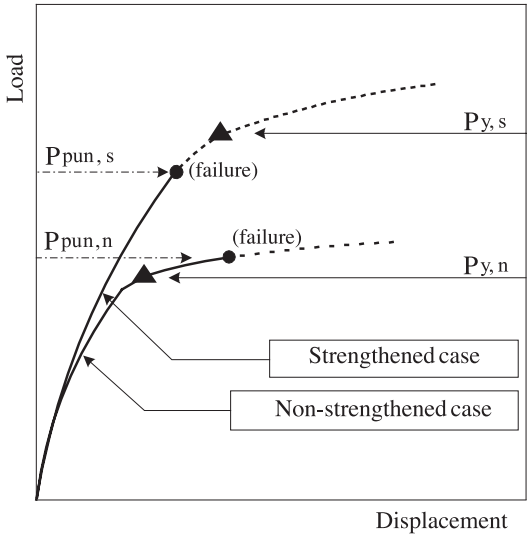

Fig. 3. The relationship between flexural strength and punching shear strength.

$$\text{Type 1}: \; P_{y,s} = 4(m_n + m_n')\frac{b_1}{l} \tag{8a}$$

$$\text{Type 2}: \; P_{y,s} = 8(m_n + m_n') \tag{8b}$$

$$\text{Type 3}: \; P_{y,s} = 4(m_n + m_n')\cot\frac{\psi}{2} + 2(m_n + m_n')\psi \tag{8c}$$

$$\text{Type 4}: \; P_{y,s} = 2(m_n + m_n')\frac{\delta}{0.5l} b\cot\frac{\psi}{2} + 2m_n\psi \tag{8d}$$

where m_n and m_n' are the positive and negative nominal yielding moments per unit width of the slab, respectively. The term $\cot\frac{\psi}{2} = \sqrt{\frac{m_n}{m_n'}}$; ψ is expressed in terms of radians.

In this method, the affinity theorem is used to determine the yield strength of orthotropic slabs such as bridge decks. An orthotropic slab can be transformed into an affine slab by the coefficient of orthotropy,

$$\mu = \frac{m_{ny}}{m_{nx}} \tag{9}$$

where m_{nx} and m_{ny} are the nominal moments per unit width in the transverse and longitudinal directions, respectively. These can be calculated in any direction as follows:

$$m_n = A_s f_y \left(d_x - 0.59\frac{A_s f_y + b_p t_p f_{psy}}{f_c'}\right) + b_{p-x} t_p f_{psy}\left(h_p - 0.59\frac{A_s f_y + b_p t_p f_{psy}}{f_c'}\right) \tag{10}$$

Here, A_s is the area of the reinforcing steel, and b_p and t_p are the width and thickness of the strengthening material. The parameter f_{psy} is the stress of the strengthening material when the reinforcements yield.

2.4. Punching shear analysis

Ménetrey proposed an analytical model to predict the punching strength of slabs [11] that was expressed in terms of the tensile strength of the concrete and the dowel action of the steel reinforcements. The effective section of the punching shear in unstrengthened slabs was assumed to be a truncated cone in shape, between 0.1d and d in slab section, because the concrete cover beneath the reinforcement can be ignored in strength analyses. However, if a strengthening material is externally bonded to the bottom of the slab, the concrete cover has a crack restraint effect due to the strengthening material [7,9]. Oh and Sim [9] extended the Ménetrey model to predict the punching strength of strengthened bridge decks, as depicted in Fig. 5. The proposed model consisted of the following equation:

$$P_{pun} = P_{c1} + P_{c2} + P_{c3} + P_{dow} + P_{anchor} \tag{11}$$

where P_{c1} is the vertical component of the tensile force from the compression side to 0.1d, P_{c2} is the vertical component of the tensile force from 0.1d to d, P_{c3} is the vertical

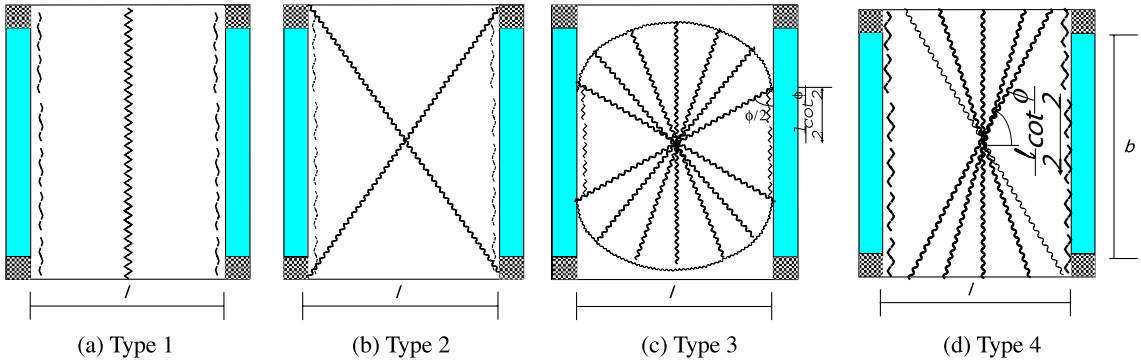

Fig. 4. Proposed yield line types of bridge decks by Sim and Oh.

component of the tensile force from d to h_p, and P_{dow} is the resistance due to the dowel effect of all bars that cross the punching crack. These terms can be expressed as

$$P_{c1} = d' f_t \cot\theta_1 [2\pi d' \cot\theta_1 + 2(a+b)]\xi\mu_a\eta \quad (12)$$

$$P_{c2} = (d-d')f_t \cot\theta_2 [2\pi(d'\cot\theta_1 + (d-d')\cot\theta_2) + 2(a+b)]\xi\mu_a\eta \quad (13)$$

$$P_{c3} = (h_p - d) f_{sp} \cot\theta_3 [2\pi(d'\cot\theta_1 + (d-d')\cot\theta_2 + (h_p-d)\cot\theta_3) + 2(a+b)]\xi'\mu_a\eta \quad (14)$$

$$P_{dow} = \frac{1}{2}\sum^{bars}\sqrt{f_c' f_y (1-\zeta^2)\sin\theta_1} \quad (15)$$

$$\sum_{n=0}^{N-n_{s1}} P_{anchor} = \sum^{N-n_{s1}} (P_{cone} + P_{bond}) \quad (16)$$

The punching strength of concrete includes the parameter ξ and ξ', which represents the influence of the percentage of reinforcing bars (ρ_s, %) and strengthening material (ρ_p, %), respectively, the size effect (μ_a), and the influence of the loaded area (η). Thus

$$\xi = \begin{cases} -0.1\rho_s^2 + 0.46\rho_s + 0.35 & \rho<0.02 \\ 0.87 & \rho\geq 0.02 \end{cases} \quad (17a)$$

$$\xi' = \begin{cases} -0.1\rho_p^2 + 0.46\rho_p + 0.35 & \rho<0.02 \\ 0.87 & \rho\geq 0.02 \end{cases} \quad (17b)$$

$$\mu_a = 1.6(1 + d/d_a)^{-1/2} \quad (18)$$

$$\eta = \begin{cases} 0.1(r_s/h_p)^2 - 0.5(r_s/h_p) + 1.25 & r_s/h<2.5 \\ 0.625 & r_s/h\geq 2.5 \end{cases} \quad (19)$$

where ϕ_s is the diameter of the reinforcing steel bars, f_s is the tensile stress in the reinforcing bar that crosses the punching crack, ρ_s and ρ_{eq} are the steel reinforcement ratio

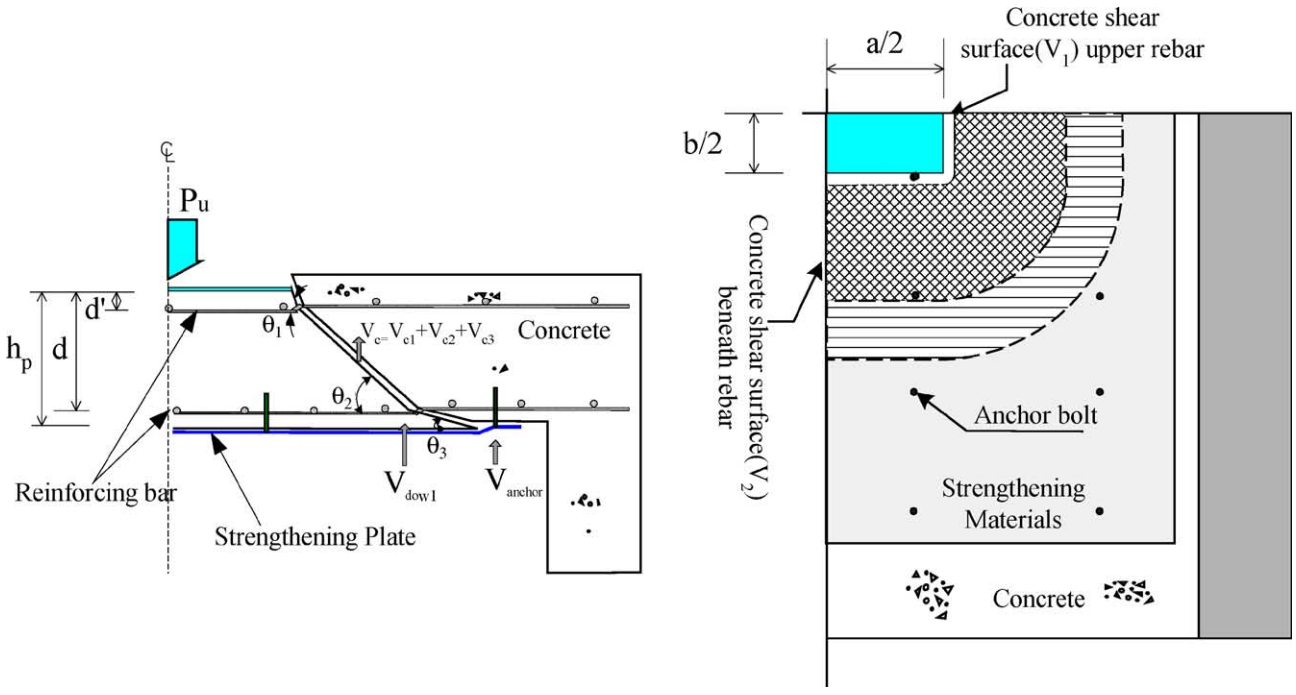

Fig. 5. Punching shear model for strengthened bridge decks.

and the equivalent strengthening ratio ($\rho_{eq}=E_p/E_s\times\rho_p$), respectively, and d_a is the maximum aggregate size. The parameter ρ_{eq} is considered only in P_{c2}. The parameter r_s is the radius of the equivalent circular loaded area, as described by Kinnunen and Nylander [4].

The tensile strength of concrete is $f_t=0.3f_c'^{2/3}$ MPa from the relationship between the compressive and tensile strengths of concrete proposed by Raphael [12]. The spalling strength of concrete is $f_{sp}=0.183\sqrt{f_c'}$ MPa (Matsui [13]) and $\zeta=f_s/f_y$. Experiments have shown that the punching crack inclination in a typical slab varies from 25 to 35° [9]. An inclination of 34°, suggested by Eurocode 2, was used for P_{c1} in the same manner as described by Ménetrey. In the strengthened slab, the crack inclination in the concrete cover was 25°, except for the one-directionally strengthened slab, for which the angle of the cracks in the bottom layer was 30°, based on the test results.

According to ACI349-85 [14], which uses the effective projected area of a stress cone, P_{cone} and P_{bond} are given by

$$P_{cone}=f_{sp}\pi\left\{\beta^2y^2-\left(\frac{D}{2}\right)^2\right\} \tag{20}$$

$$P_{bond}=u_s(l_a-x_c) \tag{21}$$

where u_s is the bond strength, y is expressed as $u+\sqrt{u^2+\frac{Du}{\beta}}+\frac{D}{2\beta}$, f_{sp} is the spalling strength of the concrete, β is tan ϕ, ϕ is the apex angle of the cone, which is equal to $(90-\theta)=55°$, x_c is the critical depth of the first cone failure, D is the diameter of the anchor bolt, and u is the length of the unbonded part.

3. Experimental results

For the experimental tests, a prototype deck panel with dimensions of 160 by 240 cm was selected to simulate a real bridge deck supported by two girders. The slab thickness was 18 cm and the 28-day compressive strength of the concrete was 22.5 MPa. The tensile rebar spacing in the transverse direction was 10 cm and the reinforcement spacing in the longitudinal direction was 15 cm. The strengthening materials used in the tests were steel plate (SP), glass fiber reinforced plastic (GP) woven in two directions, carbon fiber sheets (CS), glass fiber sheets (GS), carbon fiber rods (CFR), and grid-type carbon fiber plastic (GCFRP). An 'I' indicates that the specimen was strengthened two directionally, and 'TA' indicates that the specimen was strengthened only in the transverse direction. The test and theoretical results are summarized in Table 1.

From the test results, the load-carrying capacity of strengthened panels SP-I and GP-I, which had the greatest strengthening ratios, was 30% greater than that of the unstrengthened reference panel CON. Despite the lower strengthening ratio of panel CS-I, which was isotropically strengthened with CS strip methods to a level not more than 2% of the strengthening ratio of panel SP-I, the ultimate strength increased by 10% as compared to the reference panel CON. However, the increase in the punching shear strength was relatively small as compared to the flexural strength of the strengthened slab. Yield line theory and the punching shear model predicted the ultimate strengths of the strengthened slab systems with a reasonable degree of accuracy when compared with the test results. As reported in previous researches [1,3,4], the punching shear strength of the deck largely depended on the concrete tensile strength and the thickness of the deck, whereas the flexural strength of the deck relied on the tensile reinforcement. Therefore, if a concrete deck panel with a similar punching shear strength and flexural strength were strengthened with an externally bonded plate, the dominant failure mode of the strengthened deck would be transferred from a ductile flexural failure to a brittle punching shear failure.

However, as depicted in Fig. 6, panels SP-I, CS-TA and GCFRP-I, which were under-reinforced as compared to the maximum strengthening ratio given by Eq. (7), and were therefore expected to fail with typical flexural failure patterns, collapsed due to brittle punching shear failure in the tests. Panels CS-I and CS-TA were both under-reinforced; panel CS-I failed after structural yielding and panel CS-TA exhibited a typical punching shear failure. This proves that the transition limit of the failure pattern

Table 1
Experimental variables and results

Sepcimen	Strengthening ratio (%)		Strengthening limit criterion	Yield line theory (kN)		Punching shear strength (kN)	Test results (kN)		Failure mode
	T	L		Yields of rebar	Fracture of plate		Yields of rebar	Ultimate	
CON	–		Under-	450		635.2		633	FP
SP-I	2.5		Under-	not yield	960	810	not yield	823	P
GP-I	4.4		Over-	not yield	990	810	not yield	813	P
CS-TA	0.12	–	Under-	not yield	470	688	not yield	684	P
CS-I	0.061	0.061	Under-	620	740	712	690	732	FP
GS-I	0.65	0.65	Over-	640	840	713	600	710	P
CFR-I	0.34	0.34	Over-	not yield	1010	724	not yield	698	P
GCFRP-I	0.18	0.18	Under-	720	910	714	not yield	710	P

Here, T is transverse direction, L is longitudinal direction, FP is punching shear failure after flexural yields, and P is punching shear failure without structural yields.

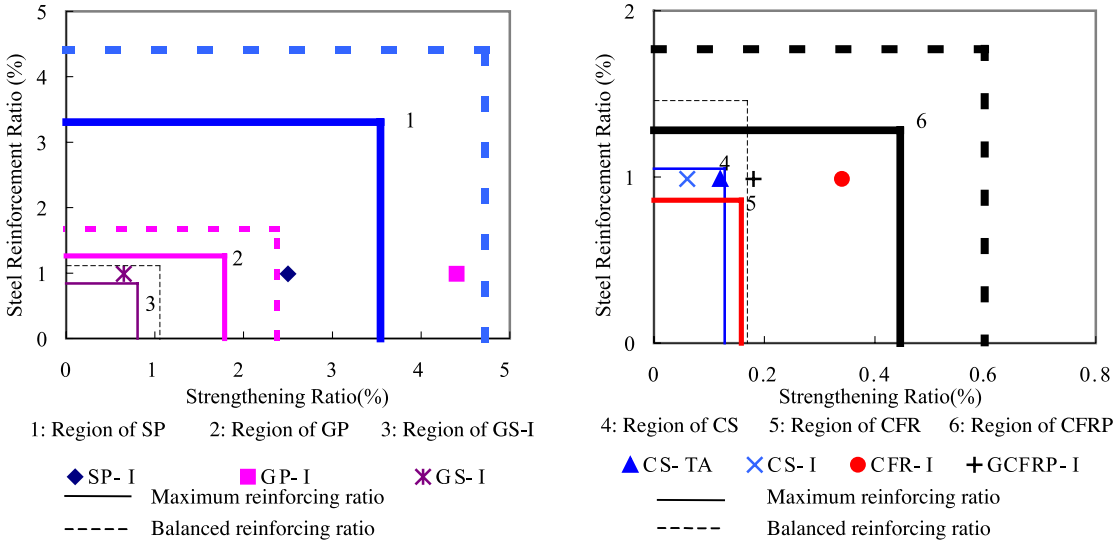

SP: steel plate, GP: glass fiber reinforced plastic woven in two directions, CS: carbon fiber sheets, GS: glass fiber sheets, CFR: carbon fiber rods, and GCFRP: grid-type carbon fiber plastic

Fig. 6. Relationship between failure mode and strengthening ratio.

changed from a flexural to punching shear in 'Region A'. The transition limit was dependent on the relationship between reinforcement ratio and strengthening ratio.

4. Strengthening limit criterion

4.1. Transition line of failure patterns

Generally in a strengthened deck, the punching strength increases less than the flexural strength. If the flexural resistance of an unstrengthened deck is slightly less than the punching resistance and the deck is strengthened using an external bonding technique, the failure mode can be changed from 'failure after the rebar yields' to 'failure before the rebar yields', as illustrated in Fig. 7. In this case,

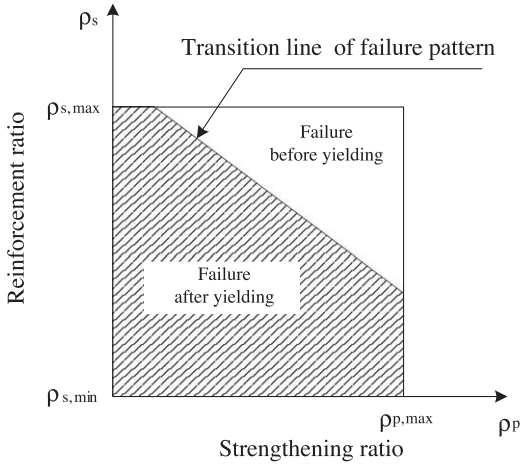

Fig. 7. Transition line of failure pattern from flexural to shear in Region A.

the strengthened deck will not be ductile, and the structural safety and necessary redundancy of the strengthened slab cannot be assured. The change of the failure pattern is defined by the 'transition line of failure pattern in 'Region A', as shown in Fig. 7.

To theoretically verify the 'transition line of failure pattern' in 'Region A', the flexural strength and punching strength of two types of strengthened bridge decks, corresponding to two design traffic loads, were analyzed using yield line theory and the extended punching shear model. The applied strengthening ratio varied from an unstrengthened case to the maximum strengthening ratio given by Eq. (7). The properties of the decks were typical of bridges for secondary design vehicles, i.e., DB-18 given by the Korea Highway Bridge Standardization [15]. The applied design traffic load for this category is similar to the HS-20 in the AASHTO design specification [16]. The specified compressive strength of the concrete was 24 MPa, and the tensile strength of the steel reinforcements was 300 MPa. The thickness of the decks was 180 mm, and the assumed loaded area was 500×250 mm, which is the same as a wheel load area. Deformed bars, #5 bars has 15.9 mm in diameter, were used to reinforce the slab panels.

The main reinforcement ratios in the transverse direction were 0.01324 per unit width for the secondary highway bridge. The percentage of longitudinal rebars was 67% of the transverse reinforcement ratio, and the amount of compressive reinforcing steel bars was half the amount of tensile rebars. The adopted strengthening material was CS, which is popular because of its good physical properties. We assumed that the CS was bonded to the bottom surface of the decks in both the longitudinal and transverse directions, and that the amount of CS in both directions was equal. The

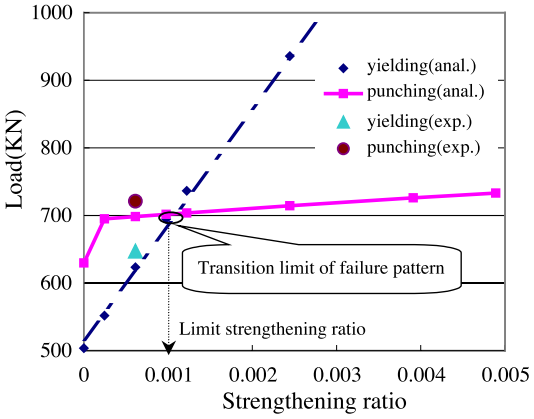

Fig. 8. Change of failure pattern by the strengthening ratio.

points indicated by 'exp.' in Fig. 8 are the test results described above.

Fig. 8 shows that the theoretical punching shear strength improved somewhat when the deck strengthening was applied using external bonding techniques without any additional enlargement of the concrete deck section. However, the flexural strength of the strengthened deck increased proportionally with the strengthening ratio until a compressive failure occurred due to over-strengthening. This suggests that the failure pattern can change from ductile yielding to brittle punching failure at the strengthening ratio where the two lines intersect, and that the strengthened deck can fail by brittle manner if the strengthening ratio is located above the transition limit in Fig. 8. To ensure a ductile failure of a strengthened bridge deck, it is desirable to use a strengthening ratio that is below the intersection point in Fig. 8 when strengthening. In this paper, we define the strengthening ratio at the intersection point as the 'strengthening limit criterion'.

Table 3
Strengthening variations for each strengthening case

Case	1st grade design traffic loads (DB-24)		2nd grade design traffic loads (DB-18)	
	Strengthening amount (cm^2/m)	Strengthening ratio	Strengthening amount (cm^2/m)	Strengthening ratio
1	–	–	–	–
2	0.33	0.00015	0.44	0.00024
3	0.66	0.00030	0.66	0.00037
4	0.99	0.00045	0.88	0.00049
5	1.32	0.00060	1.10	0.00061
6	1.65	0.00075	1.32	0.00073
7	1.98	0.00090	1.54	0.00086
8	2.20	0.00100	1.76	0.00098
9	2.64	0.00120	1.98	0.00110
10	2.97	0.00135	2.20	0.00122
11	3.30	0.00150	2.47	0.00138

4.2. Parametric analysis

In this section, bridge deck details for different reinforcement and strengthening ratios were analyzed to obtain the strengthening limit criterion. The reinforcement ratio and the strengthening ratio varied from the minimum to the maximum values given by Eq. (7). A strengthening ratio of zero indicated the unstrengthened case and the applied design traffic load DB-24 is similar to

Table 2
Design parameters of the deck applied in analysis

Case		Deck details	Rebar diameter (mm)	Main reinforcement		Distributing bar	
				Amount① (cm^2/m)	Ratio	Amount② (cm^2/m)	②/① (%)
1st grade	1	Material strength	12.7	6.335	0.003519	4.223	67
	2	(MPa): f'_c=26.5,	12.7	7.240	0.004022	5.068	70
	3	f_y=392.2;	12.7	8.447	0.004693	5.631	67
	4	Thickness/Eff.	12.7	10.136	0.005631	7.039	69
	5	depth (mm):	12.7	10.558	0.005866	7.240	68
	6	220/180	12.7	12.670	0.007039	8.447	67
	7		15.9	13.240	0.007356	8.827	67
	8		15.9	14.186	0.007881	9.930	70
	9		15.9	15.888	0.008827	11.033	69
	10		15.9	16.550	0.009194	11.348	68
	11		19.1	17.906	0.009948	11.937	67
2nd grade	1	Material strength	12.7	6.335	0.004223	4.223	67
	2	(MPa): f'_c=23.5,	12.7	7.240	0.004827	5.068	70
	3	f_y=294.2;	12.7	8.447	0.005631	5.631	67
	4	Thickness/Eff.	12.7	10.136	0.006757	7.039	69
	5	depth (mm):	12.7	10.558	0.007039	7.240	68
	6	180/150	12.7	12.670	0.008447	8.447	67
	7		15.9	13.240	0.008827	8.827	67
	8		15.9	14.186	0.009457	9.930	70
	9		15.9	15.888	0.010592	11.033	69
	10		15.9	16.550	0.011033	11.348	68
	11		19.1	17.906	0.011938	11.937	67

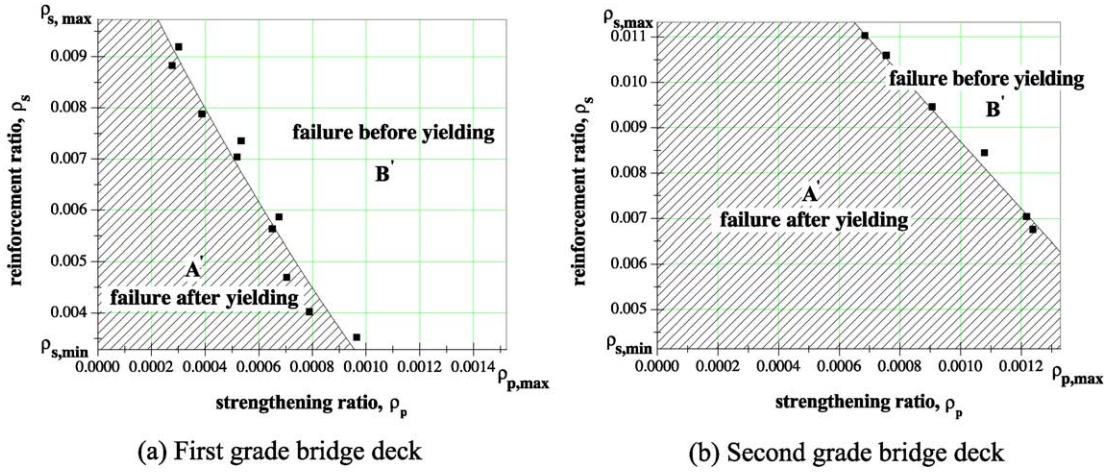

Fig. 9. Strengthening limit criterion for strengthening of bridge deck.

the HS-25. The details that were considered are summarized in Tables 2 and 3.

The results of an analysis of the strengthening limit criterion corresponding to each reinforcement ratio are shown in Fig. 9. 'Region B' is larger than 'Region A' in Fig. 9(a), which indicates that the strengthening ratio for first grade decks restricts the range of the maximum strengthening ratio to assure the flexural failure of strengthened deck. However, 'Region A' is also larger than 'Region B' in Fig. 9(b), and the strengthening ratio for second grade decks is greater. Therefore, it is more useful to strengthen second grade decks from the viewpoint of the failure patterns and strengthening effect.

5. Conclusions

The structural behavior of bridge decks changes after strengthening; therefore, the relationship between the reinforcement ratio and the strengthening limit criterion must be considered in the strengthening design procedure. This research presented a parametric study using yield line theory and a punching shear model to obtain the transition limit of failure patterns between the range of the minimum and maximum reinforcement ratios.

The increase of the flexural strength and the punching shear strength due to an external bonding technique are quite different. An analysis was performed to obtain the 'strengthening limit criterion' between the range of the minimum reinforcement and maximum strengthening ratios.

We recommend selecting a strengthening ratio in the design procedure that is less than the strengthening limit criterion. With such a selection, the load-carrying capacity of bridge decks can be sufficiently increased to support higher vehicle loads, as demonstrated by this study.

References

[1] A.K. Azad, M. Baluch, M.S.A. Abbasi, K. Kareem, Punching capacity of deck slabs in girder-slab bridges, ACI Structural Journal 91 (6) (1994) 656–662.
[2] H. Takeshi, An outline of repairing and strengthening of RC deck slabs, Bridge and Foundation Engineering 26 (8) (1994) 105–108.
[3] I.K. Fang, J.A. Worley, N.H. Burns, R.E. Klingner, Behavior of isotropic R/C bridge decks on steel girders, Journal of Structural Engineering, ASCE 116 (3) (1990) 659–678.
[4] S. Kinnunen, H. Nylander, Punching of concrete slabs without shear reinforcement, Transactions, vol. 158, Royal Institution of Technology, Stockholm, 1960.
[5] A.A. Mufti, L.G. Jaeger, B. Bakht, L.D. Wegner, Experimental investigation of fibre-reinforced concrete deck without internal steel reinforcement, Canadian Journal of Civil Engineering 20 (3) (1993) 398–406.
[6] A. Kumar, A.A. Odeh, J.R. Myers, Repair, Evaluation, Maintenance and Rehabilitation Research Program. Technical Report, Construction Engineering Research Lab. (Army), Champaign, IL, USA, 1990.
[7] H. Oh, Strengthening Design Method of Bridge Deck Reinforced by Carbon Fiber Sheet, PhD Thesis, Hanyang University, Korea, 2001.
[8] H. Oh, J. Sim, C. Meyer, Experimental assessment of bridge deck panels strengthened with carbon fiber sheets, Composites. Part B, Engineering 34 (6) (2003) 527–538.
[9] H. Oh, J. Sim, Punching shear strength of strengthened deck panels with externally bonded plates", Composites. Part B, Engineering 35 (4) (2004) 313–321.
[10] I.H. Bae, Flexural Analysis and Design of R/C Beams Strengthened with Steel Plate or Carbon Fiber Composites. PhD Thesis, Hanyang University, Korea, 1998.
[11] Ph. Menérey, Analytical computation of the punching strength of reinforced concrete, ACI Structural Journal 93 (5) (1996) 503–511.
[12] J.M. Raphael, Tensile Strength of Concrete, ACI Material Journal 81 (2) (1984) 158–165.
[13] S. Matsui, Estimation of punching shear strength of reinforced concrete bridge deck, Journal of JSCE (1984) 134–141 (in Japanese).
[14] ACI, ACI349-85 Code Requirements for Nuclear Safety Related Structures. American Institute of Concrete, 1985.
[15] Korea's Ministry of Construction and Transportation. Korean Highway Design Specification, Korea, 1996.
[16] American Association of State Highway and Transportation Officials, Standard Specifications for Highway Bridges, 16th Edition, AASHTO, Washington, DC, 1996.